Available online at www.sciencedirect.com
ScienceDirect
Cement & Concrete Composites 28 (2006) 742–748
Cement & Concrete Composites
www.elsevier.com/locate/cemconcomp

FRP debonding from a concrete substrate: Some recent findings against conventional belief

Christopher K.Y. Leung *

Department of Civil Engineering, Hong Kong University of Science and Technology, Clear Water Bay, Kowloon, Hong Kong

Available online 30 June 2006

Abstract

For beams strengthened with FRP plates, many existing theories and concepts related to debonding failure are challenged by recent experimental observations in our laboratory. For debonding initiated by stress concentrations at the plate end, ultimate failure is always preceded by the formation of a major crack in the concrete member, causing interfacial stresses to change significantly from the elastic distribution. Existing elastic models are therefore not applicable to failure prediction. For debonding initiated from a flexural crack near mid-span, fracture mechanics based models indicate that the plate stress at failure is inversely proportional to the square root of the thickness. Test results from beams of various sizes and retrofitted with plates of different thickness show a different trend. To delay debonding failure, bonding of U-shape FRP 'stirrups' to the end of the FRP plate has been proposed. Test results indicate that 'stirrups' applied away from the plate end can indeed be more effective under some practical situations.

Keywords: Composite; FRP retrofitting; Concrete beam; Debonding

1. Introduction

After years in service, many concrete structures have degraded and need to be repaired. In some cases, the structure has to be strengthened to accommodate the present load demand, which can be much higher than that when it was first constructed. For concrete beams and slabs, both laboratory and site investigations have demonstrated the bonding of fiber reinforced plastic (FRP) plates to be an effective strengthening technique. For the strengthened beam (or slab), depending on the combination of parameters (such as beam size, steel reinforcement ratio, FRP properties and dimensions, etc.), failure may occur in different modes [1–3]. When failure is due to concrete crushing (with or without yielding of the steel), or rupture of the FRP plate, the failure load can be obtained from conventional section analysis for reinforced concrete members [4,5]. However, more commonly, failure is found to result from the debonding (or separation) of the plate from the concrete [6,7]. According to a wide range of experimental observations, debonding may either initiate at the end (or cut-off point) of the FRP plate and propagate inwards, or at the bottom of a flexural or shear/flexural crack of the concrete member and propagate towards the plate end. In the former case, failure usually involves the separation of the whole concrete cover from the rest of the member [8,9]. In the latter case, the debonded FRP usually carries with it a thin layer of concrete of several mm's in thickness, indicating that failure is occurring inside the concrete substrate [7,10].

To predict debonding failure at the plate end, both the Coulomb criterion, involving the interfacial shear and normal stresses [11,12], and the biaxial principal stress criterion, involving the interfacial stresses and the longitudinal stress in concrete adjacent to the interface [13,14], have been employed. To find the interfacial stresses, different equations have been derived in various investigations [15–19], based on elastic analysis of the strengthened

* Tel.: +852 2358 8183; fax: +852 2358 1534.
E-mail address: ckleung@ust.hk

0958-9465/$ - see front matter © 2006 Elsevier Ltd. All rights reserved.
doi:10.1016/j.cemconcomp.2006.05.015

member. In some cases, the reduced moment of inertia of the concrete member is employed to account for the effect of cracking. However, the 'cracked' concrete is still taken to be elastic (with reduced modulus) and the effect of discrete cracks near the plate end has never been studied. It appears that many researchers believe that failure is indeed governed by the elastic stresses, as many recent papers [16–19] are still attempting to develop better approaches to perform the elastic analysis. In the next section of this paper, we will present experiment results to show that cracking at the plate end occurs well before the load capacity of the strengthened member is reached. Once plate end cracking occurs, the interfacial stress distribution changes significantly from the elastic case. Implications to failure prediction are discussed.

When debonding failure initiates from the bottom of a flexural or shear/flexural crack, the problem is often analyzed as the propagation of an interfacial crack when the FRP plate is pulled below the flexural crack. Various investigators [20–23] have proposed fracture mechanics based models for the analysis of crack-induced debonding. Despite the difference in details of the various models, they all predict the maximum debonding stress to decrease approximately with the square root of the plate thickness. Such a theoretical trend has never been systematically assessed with experimental results. In the third section of this paper, we will describe a testing program to study the effect of FRP plate thickness on crack-induced debonding in members of various sizes. The trend of the experimental results will be compared to the prediction from existing theoretical models.

To improve the resistance against debonding failure, U-shape FRP 'stirrups' can be applied. In Section 7.2.1.3 of the *fib* report on "Externally bonded FRP reinforcement for Reinforced Concrete Structures" [24], the following statement was made: "Anchoring of externally bonded reinforcement can be ensured by applying bonded FRP 'stirrups' that enclose the longitudinal strips at their ends ... these stirrups are not considered to be part of the shear reinforcement but are responsible to keep the longitudinal strips in their position and to prevent peeling-off." According to this recommendation, FRP 'stirrup' should be applied at the plate end. To see if this statement is generally correct, experiments are performed with FRP 'stirrups' applied at different locations along the plate. Results are presented in the fourth section of the paper.

2. Effect of cracking on stresses near the plate end

In this section, we will focus on debonding failure at the end of the FRP plate. To illustrate this failure mode, the photograph of a typical specimen is shown in Fig. 1. For this particular specimen, the reinforced concrete beam is 150 mm (Width) × 400 mm (Depth) in cross-section and supported over a span of 3.6 m. It is retrofitted with a Carbon FRP (CFRP) Plate of 0.44 mm in thickness, terminated very close to each support. According to the manufacturer, the Elastic modulus of the CFRP is 235 GPa and the strength is 4.2 GPa. Equal loading is applied through four points along the beam, placed symmetrically at 0.6 m and 1.0 m from the centerline. For the particular ratio of shear force to moment introduced by this loading configuration, failure occurs by plate end debonding. In this case, the ultimate failure load is 341 kN. At a load of 260 kN (slightly over three quarters of the failure load), an inclined crack can be clearly observed to propagate upwards from the termination point of the FRP plate. Simple calculation shows that the bending moment at the

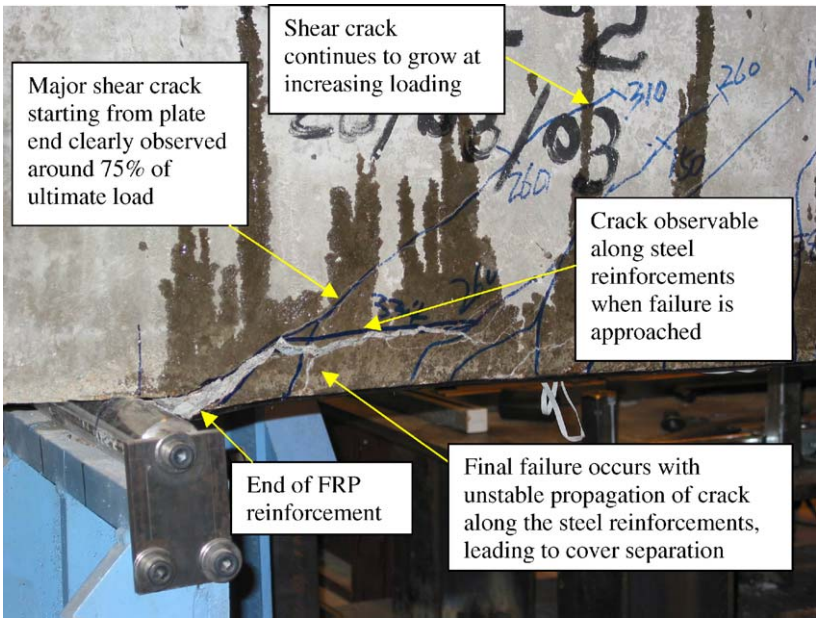

Fig. 1. Debonding failure at the plate end.

section is not high enough to cause flexural cracking. The crack is therefore initiated by high local stresses at the plate end, and propagates under the effect of shear force near the support. On further loading, the shear crack will continue to propagate (see Fig. 1). When the failure load is approached (at 332 kN), a fine horizontal crack is found at the level of the steel reinforcements. At failure, the unstable propagation of this crack causes the concrete cover to separate from the rest of the member.

The beam member in Fig. 1 has been over-reinforced with stirrups to ensure that ultimate failure will not occur in shear. Therefore, shear cracking is not the direct cause of beam failure, but the formation of a crack at the plate end is expected to affect the debonding failure load through its effect on the plate end stress distribution.

To study the effect of cracking on interfacial shear stress distribution, strain gauges were placed along the bottom of the FRP plate. Knowing the variation of strain (ε) with position (x) along the FRP plate, the interfacial shear stress (τ) can be calculated from the following equation:

$$\tau = t_p E_p \frac{d\varepsilon}{dx} \quad (1)$$

where t_p and E_p are respectively the thickness and Young's modulus of the FRP plate. Note that Eq. (1) is derived from force equilibrium and applies whether cracks are present along the concrete member or not.

As strain values are only available at a finite number of gauge points, τ has to be obtained with a numerical approach. Noting that the strain has to be zero right at the end of the plate, the central difference method is employed to calculate the interfacial shear strain at each gauge point. For the specimen shown in Fig. 1, the computed shear stress distribution is shown in Fig. 2. While numerical differentiation based on measurements at a finite number of points will not produce exact stress values, the overall trend of the results should still be reliable. From Fig. 2, for a load value up to 260 kN, the interfacial shear stress is found to increase rapidly when the plate end is approached. This observation is consistent with the results of elastic analysis [15–19]. However, with further increase in loading ($P = 270$ kN onwards), a completely different shear stress distribution can be observed as shown in Fig. 2. The stress near the plate is significantly reduced. This can be explained by the formation of a major crack at the plate end, which causes unloading of longitudinal tension in the concrete, and reduction in interfacial shear stress. The transfer of loading from the concrete to the plate then becomes much more gradual. Instead of having concentrated shear stresses at the plate end, the shear stress is distributed over a much longer distance along the plate, with maximum value occurring at a distance from the end. The experimental results indicate that once cracking occurs at the plate end, the shear stress distribution obtained from an elastic analysis is no longer applicable. Note that we have deliberately shown the results for a specimen with the plate terminated close to the support. Even for this case, plate end cracking occurs at only about 75% of the ultimate load. When the plate is terminated farther away from the support, plate end cracking will occur earlier, making the applicability of elastic analysis even more limited.

To confirm the above experimental observation, finite element analysis has also been performed to study the effect of plate end cracking on the stress distribution along the interface. Two cases, one with no crack in the concrete member and one with a discrete crack extending from the end of the FRP plate into the concrete, are analysed with the same mesh refinement. For the latter case, an inclined crack with its tip at half of the beam depth is put in the model. Through the analysis, the effect of plate end cracking on both the interfacial shear stress and interfacial

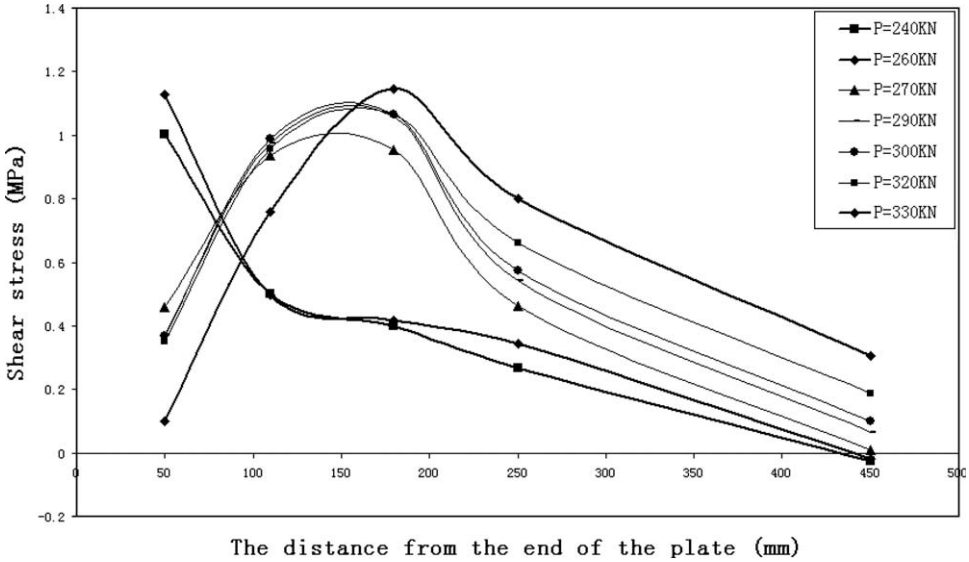

Fig. 2. Variation of interfacial shear stress obtained from numerical differentiation of experimental data.

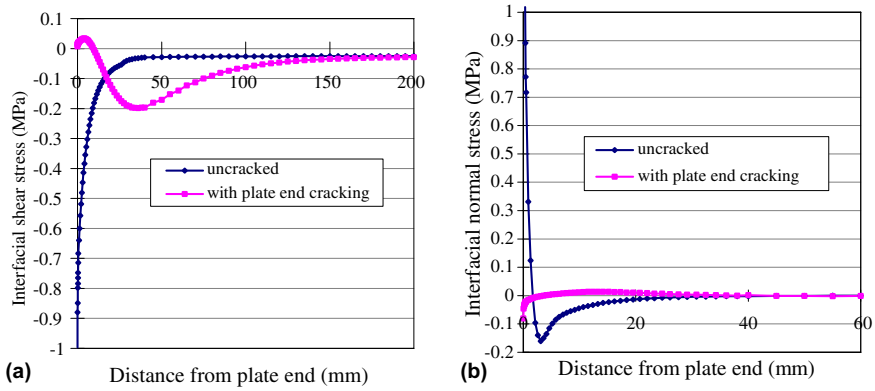

Fig. 3. Interfacial shear and normal stresses from finite element analysis.

normal stress can be obtained. The results are shown in Fig. 3. From Fig. 3(a), the interfacial shear stress for the uncracked case is found to exhibit a concentration at the plate end, and decreases rapidly with distance from it. However, as shown in the figure, when there is a crack formed at the plate end, the stress concentration disappears, and the shear stresses at locations away from the plate end are increased. This theoretical trend is in agreement with the experimental results in Fig. 2 above. Also, as shown in Fig. 3(b), high interfacial normal stress occurs at the plate end when there is no cracking. However, once cracking occurs, the normal stress concentration is no longer present. Indeed, the normal stress decreases to very small values along the interface. Since stresses of such small magnitudes are unlikely to have significant effect on the ultimate failure of the strengthened member, they can probably be neglected in the analysis of debonding failure at the plate end. It should be pointed out that the finite element results for the 'cracked' case are obtained from a mesh with a single inclined crack inside the concrete, and the final debonding of concrete cover due to the propagation of a horizontal crack along steel reinforcements (as shown in Fig. 1) has not been analysed. The results indicate that even before the occurrence of the actual debonding process, the formation of a shear crack at the plate end already induces a significant change in the stress distribution along the plate.

In summary, experimental observations indicate that plate end debonding failure is preceded by the formation of a discrete shear crack at the plate end. Once the crack is formed, the shear and normal stress concentrations predicted by elastic analysis will both disappear. Indeed, the stress transfer mechanism is completely different, and the post-cracking stress distribution has no resemblance to the elastic distribution before cracking occurs. There is hence no theoretical ground to compute the failure load from stresses obtained by elastic analysis. For the proper modelling of debonding failure at the plate end, the actual failure mechanism needs to be considered instead.

3. Effect of plate thickness on crack-induced debonding

When a flexural or shear/flexural crack tends to open at the bottom of the beam, high interfacial shear stress will be induced along the interface to initiate debonding (Fig. 4(a)). Once debonding has started, the pulling force on the plate will provide the driving force for the debonded zone to grow in size. Based on experimental observations from beam specimens under four-point loading (which is the most commonly adopted testing configuration), debonding always initiates under the crack closest to the loading point, where the moment is highest. To model crack-induced debonding, a common approach is to construct a simple model for the part of the member beyond the major crack (Fig. 4(b)). A force is applied to the plate, and the debonding process is analyzed as the propagation of a crack along the concrete/FRP interface. In most existing models, bending of the concrete specimen is neglected. In a recent paper by Leung and Tung [25], it was shown that the incorporation or neglecting of the bending effect would produce similar results.

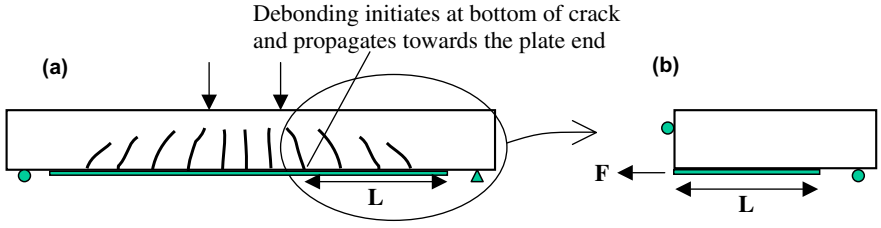

Fig. 4. Crack-induced debonding and the corresponding model for analysis.

One of the first models for FRP debonding was developed by Taljstan [20] using a nonlinear fracture mechanics approach. The force F_{db} to cause debonding failure in a sufficiently long FRP plate was derived as

$$F_{db} = b\sqrt{\frac{2E_p t_p G_{II}}{1+\alpha}} \tag{2}$$

where b, t_p and E_p are respectively the width, thickness and Young's modulus of the FRP plate. G_{II} is the interfacial fracture energy for mode II crack propagation. Also,

$$\alpha = \frac{E_p t_p}{E_c t_c} \tag{3}$$

where E_c and t_c are the Young's modulus and thickness of the concrete member. α is hence the relative stiffness between the FRP plate and the concrete member (assuming the plate and the member to have the same width).

In the same paper by Taljstan [20], assuming linear decrease of shear stress with interfacial sliding along the debonding zone, the variation of ultimate debonding force with plate length was also derived. In this case, Eq. (2) is still applicable to the prediction of debonding failure as long as the FRP plate is beyond the critical length (L_c) for full development of the softening zone. Since most models [20,21,23] indicate that L_c is only several hundred times the plate thickness, the plate length L (beyond the critical crack) in most strengthened members is beyond L_c. In the following discussions, we will therefore focus on the case with $L > L_c$. For this case, Neubauer and Rostasy [21] showed that

$$F_{db} = 0.64 k_p b\sqrt{E_p t_p f_{ctm}} \tag{4}$$

where f_{ctm} is the surface tensile strength of the concrete determined in a pull-off test. Also, k_p is a factor accounting for the width ratio between the plate and the beam. In Neubauer and Rostasy's model, the interfacial fracture energy is assumed to be proportional to f_{ctm}. Also, since the stiffness of the FRP plate is usually very small compared to the beam stiffness, the factor α is neglected. The constant 0.64 is determined from the fitting of experimental data.

A similar model has also been proposed by Chen and Teng [23]. With the theoretical solution for FRP debonding derived by Yuan and Wu [22], fitting of experimental data gives the following expression for the maximum debonding force ($L > L_c$)

$$F_{db} = 0.4\beta_p b\sqrt{E_p t_p \sqrt{f_c}} \tag{5}$$

where f_c is the concrete compressive strength obtained from a cylinder. Note that β_p is a width correction factor, slightly different in form to that given by Neubauer and Rostasy [21].

An important point to note from all the above models is that the maximum FRP stress (or strain) for debonding to occur, which is given by F_{db}/bt_p (or $F_{db}/E_p bt_p$), is inversely proportional to the square root of the plate thickness. (Note: since α is usually small compared to one, it can be neglected in Eq. (2)) Such a drastic reduction in debonding stress will significantly affect the strengthening effect of the bonded plate. While small laboratory specimens can be effectively strengthened with thin plates, the repair method may not be effective for large members employed in real structures, where much thicker plates are required. Despite the important implication of this theoretical prediction to beam strengthening in practice, no systematic tests have been performed to verify its validity. We have therefore decided to perform a series of tests to study the effect of plate thickness on debonding in beams of various sizes.

In the testing program, geometrically similar concrete beams of three different sizes are employed. These include small beams of 75 mm (W) × 200 mm (D) × 1800 mm (L), medium-size beams of $150 \times 400 \times 3600$ mm and large beams of $300 \times 800 \times 7200$ mm. The steel reinforcement ratio is essentially the same (around 1%) in all the beams. L is the span between supports, and all the members are subjected to four-point loading, with equal force applied at the one-third positions along the span. To study the size effect on plate strengthening, the small, medium-size and large beams are strengthened with geometrically similar FRP plates to achieve the same FRP volume fraction in all members. Also, to see how debonding is affected by plate thickness when the beam size is constant, medium-size beams are strengthened with plates of different thicknesses. In all the retrofitted beams, the FRP width is the same as the beam width, and the plates are terminated very close (at a distance of $L/120$) to the supports. The test parameters and results are summarized in Table 1.

In the table, each specimen is notated by its size (S, M, L) and number of FRP plies (Note: thickness of each ply is 0.11 mm). In each test, strain gauges are placed along the FRP plate, and the maximum strain (which occurs within the constant moment region) is given in the table. Also shown are computed values obtained in the following manner. Based on the point on the load vs displacement curve corresponding to steel yielding, the effective yield strength of the steel reinforcement is obtained from a conventional section analysis. Knowing the steel yield strength and the failure load, the maximum FRP strain at debonding is calculated. The good agreement between experimental and computed values indicates that the strain measurement is quite reliable.

Table 1
Fiber strain at debonding failure of various beam specimens

Specimen	Size	FRP thickness (mm)	Failure load (kN)	Maximum FRP strain ($\times 10^{-6}$)	
				Experimental	Computed
S2	Small	0.22	68.6	9114	8667
S4	Small	0.44	74.4	5904	5319
M2	Medium	0.22	216.2	7254	7287
M4	Medium	0.44	239.1	6475	6276
M6	Medium	0.66	255.2	5655	5658
M8	Medium	0.88	275.9	4934	5019
L8	Large	0.88	1024.0	7197	7247
L16	Large	1.76	1097.0	4816	4919

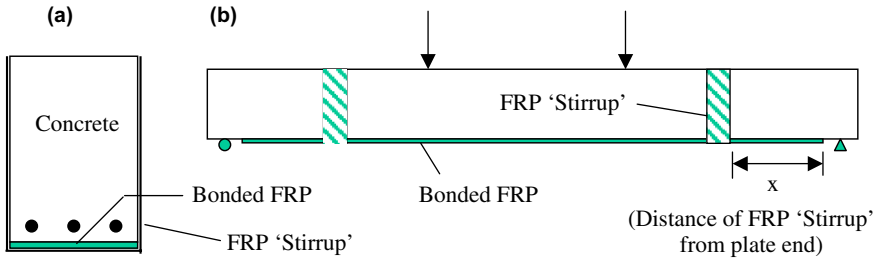

Fig. 5. (a) The FRP 'stirrup', (b) a typical specimen with FRP 'stirrup' along the plate.

To study the effect of FRP thickness on maximum debonding strain, geometrically similar specimens (S2, M4, L8, or S4, M8 and L16) are first compared. For these two sets of tests, when the FRP thickness increases by four times from the small to the large specimen, the debonding strain reduces by only about 20%. Also, the rate of reduction from the small to medium-size specimens is much more significant than that from the medium size to large members. Looking at the various medium-size beams (M2, M4, M6, M8), the FRP debonding strain does show a continuous decrease with plate thickness. However, for a four-fold increase in ply thickness, the debonding strain decreases by about one-third, rather than one-half. The inverse proportionality of debonding strain (or stress) to the square root of plate thickness, predicted by existing models, is clearly not supported by the test results.

One common problem with the models described above is that only the major crack that initiates debonding has been considered. Other cracks along the beam (as shown in Fig. 4(a)) are neglected in the model (Fig. 4(b)). Since additional cracks along the span can modify the interfacial shear stress distribution, the neglecting of such cracks may lead to erroneous prediction of the debonding force (which is in equilibrium with the interfacial shear stresses). The development of a new model that can account for multiple cracking is certainly needed.

4. Optimal location of FRP 'stirrup' along the bonded plate

To improve the resistance against debonding failure, one plausible approach is to apply an U-shaped FRP 'stirrup' (Fig. 5(a)) on top of the bonded plate. As mentioned in the Introduction, according to the recommendations in a *fib* technical report [24], the U-shaped 'stirrup' should be placed at the end of the bonded plate. However, it is not obvious to us that the plate end is always the optimal location for the FRP 'stirrup'. We have therefore conducted a series of tests with the U-shaped 'stirrup' applied at various locations along the bonded plate. A typical specimen is shown in Fig. 5(b). The size and steel reinforcement detail is exactly the same as that for the medium-size beam described in the last section. Four plies (0.44 mm) of CFRP was bonded on the bottom of the beam before two U-shaped 'stirrups' (150 mm wide, 0.22 mm thickness) are applied symmetrically on both sides of the beam. The shear span in the beam is 1.2 m, and the plate is terminated at 50 mm from each support. For various 'stirrup' locations, the results are summarized in Table 2.

Table 2
Effect of 'stirrup' location on FRP debonding failure

Specimen	Location of 'stirrup' from plate end (mm)	Failure load (kN)
Control	N/A, no 'stirrup' for the control	263.35
U1	0	263.92
U2	530	283.74
U3	750	299.24

The test results in Table 2 indicate that the load capacity of the retrofitted beam increases when the FRP 'stirrup' is moved away from the plate end. Indeed, by placing the 'stirrup' right at the plate end, there is no increase in load capacity. The explanation is as follows. In all the tested specimens, debonding failure is initiated by a crack near the loading point. The debonded zone has to reach the 'stirrup' before its resistance can be activated. If the 'stirrup' is far away from the middle of the beam, the contribution of the 'stirrup' to the total bond force is compromised by the decreasing load carrying capacity along the debonded interface due to shear softening. To maximize the total load carrying capacity, the 'stirrup' should be placed close to the initiation point of debonding, so the stirrup's resistance is activated before significant debonding (and interfacial softening) has occurred.

In our experiments, debonding is initiated near the mid-span. It is of course possible for debonding to initiate at the end of the FRP plate, as shown in Fig. 1. Under such a situation, a FRP 'stirrup' at the plate end may be effective in increasing the FRP debonding load. However, our results indicate that it is not always beneficial to put the FRP 'stirrup' at the plate end, so the recommendation stated in the *fib* report is not always appropriate.

5. Conclusion

In this paper, experimental results are presented to show that several common believes related to debonding failure in FRP strengthened concrete beams are not correct. Specifically, for plate end debonding, a physically sound

failure criterion should not be based on elastic stresses. When debonding initiates from a crack at the middle of the beam, the drastic decrease of debonding stress with plate thickness, predicted by existing models, is not found in real specimens. Also, when FRP 'stirrups' are used to increase resistance to debonding, the recommended practice to apply the 'stirrup' at the plate end is not necessarily appropriate. We are hoping that the findings in this paper can provide useful information for future research and design recommendations related to the debonding failure in FRP strengthened concrete beams.

References

[1] Meier U. Strengthening of structures using carbon fibre/epoxy composites. Construct Build Mater 1995;9(6):341–53.
[2] Arduini M, Di Tommaso A, Nanni A. Brittle failure in FRP plate and sheet bonded beams. ACI Struct J 1997;94(4):363–70.
[3] Buyukozturk O, Leung C, Hearing B, Gunes O. Delamination criterion for concrete beams retrofitted with FRP laminates. In: Mihashi H, Rokugo K, editors. Fracture mechanics of concrete structures. Aedificatio Press; 1998. p. 1771–82.
[4] Wei A, Saadatmanesh H, Ehsani MR. RC beams strengthened with FRP plates II: analysis and parametric study. ASCE J Struct Eng 1991;117(11):3434–55.
[5] Triantafillou TC, Plevris N. Strengthening of R/C beams with epoxy-bonded fiber composite materials. Mater Struct 1992;25:201–11.
[6] Meier U, Deuring M, Meier H, Schwegler G. Strengthening of structures with CFRP laminates: research and applications in Switzerland. In: Advanced composite materials in bridges and structures: Canadian Society for Civil Engineering, 1992. p. 243–51.
[7] Saadatmanesh H, Ehsani MR. RC beams strengthened with FRP plates I: experimental study. ASCE J Struct Eng 1991;117(11): 3417–33.
[8] Sharif A, Al-Sulaimani GJ, Basunbul IA, Baluch MH, Ghaleb BN. Strengthening of initially loaded reinforced concrete beams using FRP plates. ACI Struct J 1994;91(2):160–8.
[9] Nguyen DM, Chan TK, Cheong HK. Brittle failure and bond development length of CFRP-concrete beams. ASCE J Compos Construct 2001;5(1):12–7.
[10] Rahami H, Hutchinson A. Concrete beams strengthened with externally bonded FRP plates. ASCE J Compos Construct 2001;5(1):44–56.
[11] Ziraba YN, Baluch MH, Basunbul IA, Azad AK, Al-Sulaimani GJ, Sharif AM. Guidelines towards the design of reinforced concrete beams with external plates. ACI Struct J 1994;91(6):639–46.
[12] Varastehpour H, Hamelin P. Strengthening of concrete beams using fiber-reinforced plastics. Mater Struct 1997;30:160–6.
[13] Saadatmanesh H, Malek AM. Design guidelines for flexural strengthening of RC beams with FRP plates. ASCE J Compos Construct 1998;2(4):158–64.
[14] El-Mihilmy M, Tedesco JW. Prediction of anchorage failure for reinforced concrete beams strengthened with fiber-reinforced polymer plates. ACI Struct J 2001;98(3):301–14.
[15] Roberts TM. Approximate analysis of shear and normal stress concentrations in the adhesive layer of plated RC beams. Struct Eng 1989;67:229–33.
[16] Taljsten B. Strengthening of beams by plate bonding. ASCE J Mater Civil Eng 1997;9(4):206–12.
[17] Malik AM, Saadatmanesh H, Ehsani MR. Prediction of failure load of R/C beams strengthened with FRP plate due to stress concentration at the plate end. ACI Struct J 1998;95(1):142–52.
[18] Rabinovich O, Frostig Y. Closed-form higher-order analysis of RC beams strengthened with FRP strips. ASCE J Compos Construct 2000;4(1):65–74.
[19] Shen HS, Teng JG, Yang J. Interfacial stresses in beams and slabs bonded with thin plate. ASCE J Eng Mech 2001;127(4):399–406.
[20] Taljsten B. Strengthening of concrete prism using the plate-bonding technique. Int J Fract 1996;82:253–66.
[21] Neubauer U, Rostasy FS. Design aspects of concrete structures strengthened with externally bonded CFRP plates. In: Forde MC, editor. Structural faults and repairs-97, 1997. p. 109–18.
[22] Yuan H, Wu Z. Interfacial fracture theory in structures strengthened with composite of continuous fiber. In: Proceedings of symposium of china and japan, science and technology of 21st Century, Tokyo, Japan, 1999. p. 142–55.
[23] Chen JF, Teng JG. Anchorage strength models for FRP and steel plates attached to concrete. ASCE J Struct Eng 2001;127(7):784–91.
[24] fib Task Group 9.3. Externally bonded FRP reinforcement for RC structures. Technical Report 2001.
[25] Leung CKY, Tung WK. Three-parameter model for debonding of FRP plate from concrete substrate. ASCE J Eng Mech 2006;132(5): 509–18.